An Assessment of the Role of Quenched Randomness in the Stereochemical Sequences of Atactic Vinyl Polymers

Wayne L. Mattice and Numan Waheed*

Institute of Polymer Science, The University of Akron, Akron, Ohio 44325-3909

Received November 14, 2005; Revised Manuscript Received January 10, 2006

ABSTRACT: The influence of the quenched randomness in the stereochemical sequences of atactic chains on the mean-square unperturbed end-to-end distance, $\langle r^2\rangle_0$, is assessed. The method uses a rotational isomeric state (RIS) model based on virtual bonds between the centers of mass of the C_6 rings in polystyrene. This virtual bond model is derived from a conventional RIS model expressed in terms of the C−C bonds in the main chain. The zeroth-approximation virtual bond model, which retains only the most probable conformations of each tetrad, correctly finds $\langle r^2\rangle_0 \sim n$ in the limit as $n \rightarrow \infty$ if the probability for a *meso* diad, p_m, is $0 < p_m < 1$, although the same zeroth-approximation model yields $\langle r^2\rangle_0 \sim n^2$ if p_m is either 0 or 1. The values of $\langle r^2\rangle_0$ at intermediate p_m are surprisingly close to the ones deduced from a full, C−C bond based RIS model. This achievement of the zeroth-approximation model demonstrates the important role of the quenched randomness of the stereochemical sequences in determining the unperturbed dimensions of atactic chains. Excellent agreement with the $\langle r^2\rangle_0$ from the full RIS model based on C−C bonds over the entire range of stereochemical composition, $0 \le p_m \le 1$, can be achieved in a first-approximation virtual bond model, which includes the next most probable conformations at each tetrad and refines slightly some of the conformations by minor adjustments in soft degrees of freedom.

Introduction

Quenched randomness in the stereochemical sequence of atactic vinyl polymers causes samples with intermediate stereochemical composition ($0 < p_m < 1$, where p_m denotes the probability of a *meso* diad) to be fundamentally different from samples at the extremes of stereochemical composition, where p_m is either 0 or 1. At the extremes, a single conformational partition function, *Z*, describes all of the chains in a stereochemically monodisperse sample. However, for mixtures of intermediate stereochemical composition, an enormous number of different *Z*'s apply, even when all of the chains have the same number of bonds, *n*. If *n* is large, it is unlikely that any two chains in an atactic sample have the same *Z*. For this reason, Flory noted that vinyl polymers with intermediate stereochemical composition are properly considered as copolymers.[1] While models of the randomness of stereochemistry in atactic chains are new, the general study of quenched randomness using statistical mechanics approaches has been of long-standing interest, not only in characterizing random copolymers[2] but also in the treatment of the random physical cross-links in rubber-elasticity theory[3] and of the random-ordered ground state in spin glasses.[4]

One manifestation of this fundamental difference between the stereochemically pure and atactic vinyl polymers is the minimum requirement for the anticipated asymptotic behavior of the mean-square unperturbed end-to-end distance, $\langle r^2\rangle_0$. If segments of a stereochemically pure chain repeat the same conformation, the long chain describes a helix for which $\langle r^2\rangle_0 \sim n^2$ in the limit as $n \rightarrow \infty$. This expectation might be qualitatively different if the stereochemically pure chain is replaced by an atactic polymer. If the most probable conformation is assigned to each diad in an atactic polymer, the asymptotic limit will be $\langle r^2\rangle_0 \sim n$ if the quenched randomness in the stereochemical sequence is sufficient to prevent the propagation of the same conformation everywhere along the contour of the chain. This qualitative argument leads to the speculation that the quenched randomness in the stereochemical sequence might by itself be sufficient to account qualitatively for the dependence of $\langle r^2\rangle_0$ on p_m at intermediate values of p_m. Here we evaluate this speculation, using polystyrene (PS) as the specific system for investigation.

The method employed for the analysis provides an entrée to the development of more robust simulations of dense systems of polymers with bulky side chains. It is well-known that the time scales involved in the equilibration of dense melts of polymers of high degree of polymerization are not easily reached with simulations in which chains are represented with full atomistic detail. This fact is responsible for the widespread use of coarse-grained chains in the simulation of polymer melts.[5] Coarse-grained chains are ideally suited to the investigation of universal properties, where atomistic detail is not important. However, if the objective is information about a specific polymer, it becomes important to construct the coarse-grained model in a manner that permits an unambiguous connection with the real chain of interest. This objective can be achieved by the imposition of constraints on the coarse-grained chains.[6]

The rotational isomeric state (RIS) model has played an important role in the construction of constraints that facilitate the recovery of full atomistic detail from equilibrated coarse-grained models.[6] RIS models are frequently expressed in terms of the covalent bonds in the main chain of the polymer, although sometimes the covalent bonds are replaced by virtual bonds.[7−9] For most simple polymers, RIS models utilize values for the bond length, l, bond angle, θ, torsion angles, ϕ, and short-range hindrances to the torsion potentials that can be deduced from the properties of small molecules. For example, the relevant structural and energetic information for an RIS model for polyethylene can be derived from *n*-butane and *n*-pentane.[10] The conventional RIS model, expressed in terms of the covalent bonds in the backbone, can be mapped onto another RIS model that describes coarse-grained beads situated at the sites of alternate backbone atoms.[11] The parent RIS model then controls the distribution function for the end-to-end vector for the coarse-grained chain and all of its subchains. This approach, with one

10.1021/ma052434q CCC: $33.50 © 2006 American Chemical Society
Published on Web 02/23/2006

coarse-grained bead per monomer unit, has been successfully used for a few vinyl polymers including polypropylene[12] and PS.[13]

Since the RIS model is a single chain model, the intermolecular interactions of the coarse-grained chains in a melt must be treated separately, such as via a Lennard-Jones (LJ) potential that operates between pairs of coarse-grained beads.[14] The locations of the sites of the LJ centers for polymers with bulky side chains would be improved if they were to reside in the side chains, especially if most of the mass of the polymer resides in the side chains. The method developed here to analyze the consequences of the quenched randomness of atactic vinyl polymers also provides a method for improving the location of the coarse-grained beads that represent monomer units with bulky side chains. The method therefore provides an entrée to efficient simulation of coarse-grained models for highly decorated atactic PS (*a*PS) of the types prepared and studied by Percec,[15] Schlüter,[16] and Frechet.[17]

This article presents the general strategy, followed sequentially by implementation and assessment of that strategy for syndiotactic PS (*s*PS, $p_m = 0$), isotactic PS (*i*PS, $p_m = 1$), and *a*PS ($0 < p_m < 1$). The consequences of the quenched randomness are presented in the discussion of *a*PS.

General Strategy

Tetrads permit the mapping of a conventional RIS model, expressed in terms of C−C bonds in the main chain, onto another model expressed in terms of virtual bonds that connect the centers of successive side chains. We first present the relevant features of the conventional RIS model and then describe how this information is incorporated into the new description of PS, based on virtual bonds connecting the centers of mass of successive C_6 rings.

The $\langle r^2\rangle_0$ is written in the RIS model as the ratio of two serial products of n matrices.[18]

$$\langle r^2\rangle_0 = Z^{-1}\mathbf{F}_1...\mathbf{F}_n \tag{1}$$

$$Z = \mathbf{U}_1...\mathbf{U}_n \tag{2}$$

Here Z is the serial product of n statistical weight matrices, $\mathbf{U}_i$, with one statistical weight matrix for each bond in the chain. Each generator matrix, $\mathbf{F}_i$, incorporates all of the energetic information in $\mathbf{U}_i$, along with the bond vector, $\mathbf{l}_i$, the angle between bonds i and $i+1$, θ_i, and the torsion angle at bond i, ϕ_i, for all rotational isomers. This operation is achieved at each internal $\mathbf{F}_i$ by expansion of $\mathbf{U}_i$ through multiplying of each of its elements by a 5×5 matrix, $\mathbf{G}_i$, where θ_i and ϕ_i appear in the transformation matrix, $\mathbf{T}_i$.[18]

$$\mathbf{G}_i = \begin{bmatrix} 1 & 2\mathbf{l}_i^T\mathbf{T}_i & l_i^2 \\ 0 & \mathbf{T}_i & \mathbf{l}_i \\ 0 & 0 & 1 \end{bmatrix} \tag{3}$$

The special forms for the end vectors, F_1 and F_n, are easily obtained from the more general F_i for internal bonds.[18]

RIS models for PS began to appear in the literature in the 1960s.[19,20] These models and more recent ones[21−24] differ in notation (use of t, g^+, g^- states when the stereochemical sequence is expressed using pseudoasymmetric centers or t, g, $\bar{g}$ states when the stereochemical sequence is expressed using *meso* and *racemo* diads) and in the values assigned to θ, ϕ, and the statistical weights. For present purposes, we adopt a simple model with tetrahedral bond angles in the backbone and three torsion angles (t, g^+, g^-) separated by 120°. Each l_i is 0.154 nm, each θ_i is 109.5°, the three ϕ_i are 180° and ±60°, the internal $\mathbf{U}_i$ are of dimensions 3×3, and the internal $\mathbf{F}_i$ are of dimensions 15×15.

Describing the stereochemical sequences using *dl* pseudoasymmetric centers, as defined on p 175 of ref 5, and denoting by C^α the main chain atom directly bonded to the side chain, the $\mathbf{U}_i$ for the C^α−C bonds in PS are[19]

$$\mathbf{U}_d = \begin{bmatrix} \eta & 1 & \tau \\ \eta & 1 & \tau\omega \\ \eta & \omega & \tau \end{bmatrix} \tag{4}$$

$$\mathbf{U}_l = \mathbf{Q}\mathbf{U}_d\mathbf{Q} \tag{5}$$

$$\mathbf{Q} = \begin{bmatrix} 1 & 0 & 0 \\ 0 & 0 & 1 \\ 0 & 1 & 0 \end{bmatrix} \tag{6}$$

and the U_i and for C−C^α bonds are

$$\mathbf{U}_{dd} = \begin{bmatrix} \eta\omega_{xx} & \tau\omega_x & 1 \\ \eta & \tau\omega_x & \omega \\ \eta\omega_x & \tau\omega\omega_{xx} & \omega_x \end{bmatrix} \tag{7}$$

$$\mathbf{U}_{ll} = \mathbf{Q}\mathbf{U}_{dd}\mathbf{Q} \tag{8}$$

$$\mathbf{U}_{dl} = \begin{bmatrix} \eta & \omega_x & \tau\omega_{xx} \\ \eta\omega_x & 1 & \tau\omega \\ \eta\omega_{xx} & \omega & \tau\omega_x^2 \end{bmatrix} \tag{9}$$

$$\mathbf{U}_{ld} = \mathbf{Q}\mathbf{U}_{dl}\mathbf{Q} \tag{10}$$

The columns are indexed by the states at bond i, the rows are indexed by the states at bonds $i-1$, and the order of indexing is t, g^+, g^-. As described by Flory et al.,[19] τ is the statistical weight for a simultaneous first-order interaction of a backbone atom with the side chain and another backbone atom, η is the statistical weight for a single first-order interaction of a backbone atom and the side chain, and the ω's are statistical weights for second-order interactions (backbone−backbone for ω, backbone−side chain for ω_x, and side chain−side chain for ω_{xx}).

Now consider points lying along the direction defined by the C^α−C^{ar} bond, where C^{ar} is the atom in the side chain that is directly bonded to C^α. The center of mass of the C_6 ring is one of these points, as shown in Figure 1. In the approximation that all bond lengths and bond angles are fixed, this point is rigidly attached to the backbone, at a distance of 0.29 nm from C^α. If the stereochemical sequence of the chain is specified, the conformation defined by the n C−C bonds in the backbone unambiguously defines the conformation of the $n/2$ points representing the centers of mass of the $n/2$ rings. Virtual bonds are now drawn between the points at the center of mass of the rings, as shown in Figure 2. The length of the virtual bond depends on the stereochemical sequence of the diad and on the torsions at the two intradiad C−C backbone bonds. The angle between two successive virtual bonds depends on the stereochemical sequence of the triad and on the torsions at four consecutive C−C backbone bonds. The torsion angle about a virtual bond depends on the stereochemical sequence of a tetrad and on the conformations at six backbone C−C bonds.

All of this geometric information for the virtual bond model can be obtained from the conformations of a small molecule, 2,4,6,8-tetraphenylnonane (TPN), Figure 2, of the appropriate

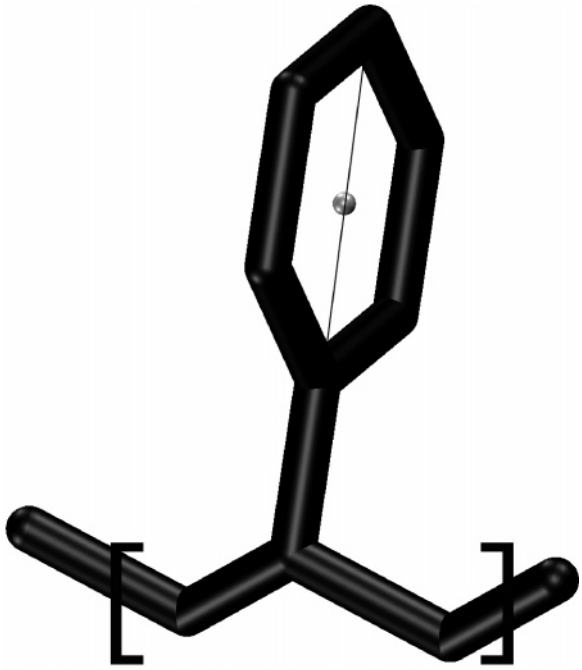

Figure 1. A small fragment of PS. The solid line is drawn along the $C^{\alpha}-C^{ar}$ bond. The filled circle on this line denotes the center of mass of the C_6 ring (image rendered using Visual Molecular Dynamics,[25] version 1.8.3).

stereochemical sequence. The statistical weight for each set of geometric information is obtained from the statistical weight of each conformation of the TPN, as determined using the matrices in eqs 4−10. This information defines the elements in a new set of statistical weight matrices for the virtual bonds. While the usual RIS treatment based on C−C bond includes only first- and second-order interactions, the present treatment incorporates interaction up to sixth order because the torsion angle at the virtual bond depends on the torsions at six consecutive C−C bonds.

If all of this weighting information is retained, the new statistical weight matrices will be huge (729×729 if three states are assigned to each internal C−C bond). Fortunately, most of this information is of little consequence because it concerns conformations of TPN that have very small statistical weights and low probability of occurrence in PS. Therefore, the new RIS model, expressed in terms of the virtual bonds between the centers of mass of the side chains, can be accurately written using surprisingly simple expressions for the statistical weight matrices. The new RIS model can be developed in a systematic approach that is illustrated below for PS but should be directly applicable to many other vinyl polymers also. This systematic approach provides insights into the role played by the quenched randomness of the stereochemical sequences in determining the conformation-dependent properties of *a*PS. Before considering *a*PS, we deal first with the simpler *s*PS and *i*PS.

Results and Discussion

Syndiotactic Polystyrene. A specific stereochemical sequence of TPN has $3^6 = 729$ conformations if three rotational isomeric states are retained for each of the six internal C−C bonds in the backbone. Only two states will be retained here because, as described by Yoon et al.,[23] the gauche state with τ in its statistical weight has an energy so high that it can safely be ignored. Rejection of this gauche state leaves $2^6 = 64$ conformations for each stereochemical sequence of TPN in the parent (C−C bond based) RIS model. Using values of the

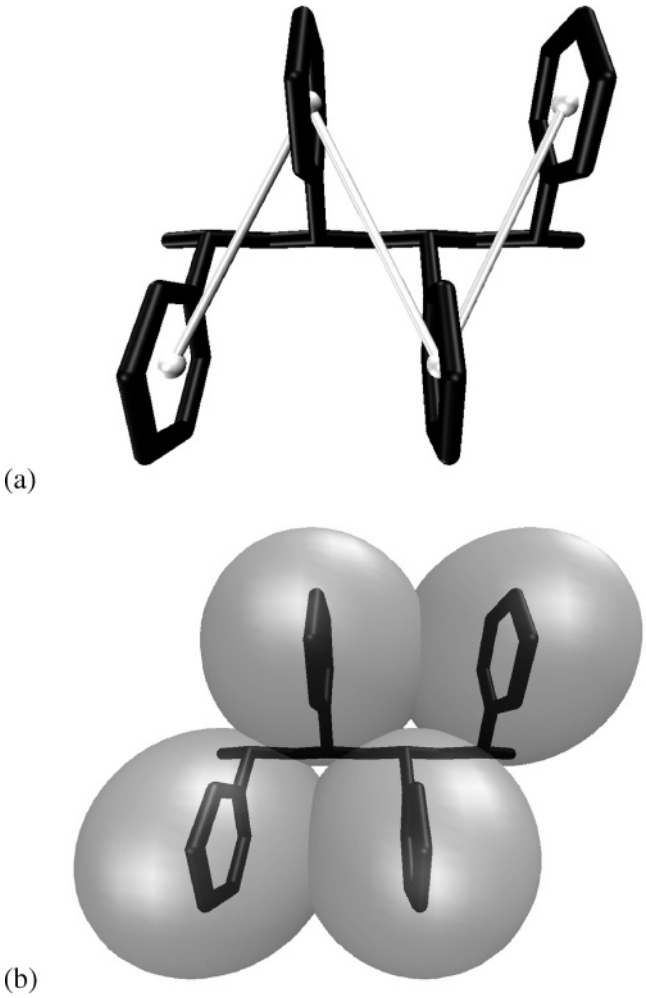

Figure 2. The most probable conformation of *s*TPN, representing a tetrad of sPS, along with the three virtual bonds that connect successive centers of the C_6 rings. Part (a) depicts all carbon atoms, along with the virtual bonds. Part (b) depicts the LJ spheres cited at the center of mass of each C6 ring, viewed from a direction parallel with the bisector of the $C^{\alpha}-C-C^{\alpha}$ angle (images rendered using Visual Molecular Dynamics,[25] version 1.8.3).

statistical weights that are appropriate for PS at a temperature of 300 K,[23] namely $\eta = 1.58$, $\omega = \omega_x = 0.047$, and $\omega_{xx} = 0.045$, syndiotactic TPN (*s*TPN) has $Z = 41.4$. Individual conformations have statistical weights that vary by a factor of 10^6. Our objective is to retain only enough conformations so that the new model, based on $n/2$ virtual bonds, yields values of $\langle r^2\rangle_0$ for a long *s*PS chain that are an adequate approximation to the values of $\langle r^2\rangle_0$ from the full RIS model based on n C−C bonds. We start with the conformation of *s*TPN of highest statistical weight and include additional conformations of successively lower statistical weight until a suitable approximation is reached. This process is facilitated by understanding how, and why, each newly incorporated conformation affects $\langle r^2\rangle_0$ for a long chain.

The *ttttt* conformation (defined in terms of the rotational isomeric states at the internal C−C bonds) is the single conformation of *s*TPN with the highest statistical weight, η^6. Its statistical weight accounts for 37.5% of *Z*. In this conformation, the virtual bond model has bond vectors with a length 0.54 nm, a bond angle of 55°, and a torsion angle of 180°. It is worthwhile to compare the length of the virtual bond with the "size", σ, that might be assigned to the LJ center for each monomer unit.

$$E_{LJ} = 4\epsilon[(\sigma/r)^{12} - (\sigma/r)^{6}] \quad (11)$$

A value of $\sigma = 0.5932$ nm was deduced from viscosity measurements for toluene, $C_6H_5CH_3$.[26] Using this result as a rough guide to the likely size of σ for the styryl repeat unit, $C_6H_5CHCH_2$, the distance between successive LJ centers in the *ttttt* conformation of the *s*PS is ~90% of σ. Furthermore, LJ centers i and $i \pm 2$ are separated by a distance that is about 84% of σ. In terms of LJ centers, the new coarse-grained model of the *ttttt* conformation of *s*PS is a string of LJ spheres in which bonded spheres slightly overlap, as do next-nearest-neighbor spheres, as shown in Figure 2. The arrangement of LJ centers in Figure 2 captures the fact that the side chains switch from one side of the main chain to the other as one proceeds along the chain. This alternating pattern would not be seen if the LJ center for each monomer unit was placed at C^{α}. Then all LJ centers would lie on a straight line, with a spacing of 0.25 nm.

The *ttttt* conformation alone provides a woefully inadequate approximation to the parent C−C bond based RIS model. The planar zigzag chain yields $\langle r^2\rangle_0 \sim n^2$ as $n \rightarrow \infty$, but the parent RIS model based on C−C bonds produces $\langle r^2\rangle_0 \sim n$ in the same limit. An acceptable virtual bond model must include higher energy (lower statistical weight) conformations that interrupt the propagation of the planar zigzag, *ttttt* conformation.

Inclusion of the conformations with the next higher statistical weight, η^4, provides for disruption of the *ttttt* sequence by isolated diads in the *gg* conformation. There are three such conformations in *s*TPN because the *gg* conformation can be placed at any of the three *racemo* diads. These gauche states are g^+g^+ if they are placed within a *dl* diad and g^-g^- if placed within an *ld* diad. Adding these conformations of *s*TPN to the *ttttt* conformation accounts for 82.6% of *Z*. The virtual bond model based on these conformations of *s*TPN correctly predicts $\langle r^2\rangle_0$ is proportional to n as $n \rightarrow \infty$. Furthermore, the values of $\langle r^2\rangle_0$ at high n are quite close (lower by only 7%) to the values for the same chain, using the full C−C bond based RIS model. The statistical weight matrix for a virtual bond from a *d* to an *l* pseudoasymmetric center in *s*PS is

$$\mathbf{U}_{dl,\text{syndio}} = \begin{bmatrix} \eta^2 & \eta^2 & 0 & 0 \\ 0 & 0 & 1 & 0 \\ 0 & 0 & 0 & \eta^2 \\ \eta^2 & \eta^2 & 0 & 0 \end{bmatrix} \quad (12)$$

The order of indexing for the columns is a^0, b^-, c^-, d^-, and the order of indexing for the rows is a^0, b^+, c^+, d^+. The signs denote the sign of the torsion angle, as shown in Table 1. $\mathbf{U}_{ld,\text{syndio}}$ is obtained from $\mathbf{U}_{dl,\text{syndio}}$ by exchanging + and − signs on all torsion angles and in the indexing of the rows and columns. Whereas Z for the long *s*PS chain in the C−C bond RIS model depends on the serial product of four matrices, $\mathbf{U}_d\mathbf{U}_{dl}\mathbf{U}_l\mathbf{U}_{ld}$, the equivalent information is now contained in the serial product of two matrices, $\mathbf{U}_{dl,\text{syndio}}\mathbf{U}_{ld,\text{syndio}}$.

Although this virtual bond model is in quite good agreement with the parent RIS model based on C−C bonds, it is worthwhile to inquire whether the agreement is significantly improved upon including the next most probable conformation of *s*TPN in the analysis. If we include this single conformation, with statistical weight η^2, the *gg* conformations need no longer be isolated as *...ttttggtttt...*, but can instead alternate with the *tt* conformations, as *...ttggttggtt...*. Inclusion of this fifth conformation of *s*TPN, namely, the *ggttgg* conformation, yields a five-conformation model that accounts for 88.6% of *Z*. The statistical weight matrix becomes

$$\mathbf{U}_{dl,\text{syndio}} = \begin{bmatrix} \eta^2 & \eta^2 & 0 & 0 & 0 \\ 0 & 0 & 1 & 0 & 0 \\ 0 & 0 & 0 & \eta^2 & \eta^2 \\ \eta^2 & \eta^2 & 0 & 0 & 0 \\ 0 & 0 & 1 & 0 & 0 \end{bmatrix} \quad (13)$$

The order of indexing for the columns is a^0, b^-, c^-, d^-, e^-, and the order of indexing for the rows is a^0, b^+, c^+, d^+, e^+.

At high n, the values of $\langle r^2\rangle_0$ obtained using virtual bonds and the statistical weight matrix in eq 13 are 5% larger than the values for the same chain using the parent RIS model based on C−C bonds. Since the simpler model, eq 12, provided values of $\langle r^2\rangle_0$ that were nearly as accurate (7% too small), it is not immediately obvious that inclusion of the extra conformation was worth the effort.

Further improvement in the quantitative agreement between the virtual bond model and the parent RIS model expressed in terms of C−C bonds could be sought by including even more conformations. If all 64 conformations of *s*TPN were included in the virtual bond RIS model, the agreement should become exact. Of course, the virtual bond RIS model would then require huge U. An equally accurate, but more tractable, model is obtained if full optimization is achieved by simply making minor changes in the soft degrees of freedom for the conformations in eq 12 that are responsible for disruption of the planar zigzag conformation. The four-state virtual bond model yields values of $\langle r^2\rangle_0$ at high n that are indistinguishable from those of the parent C−C bond based RIS model if the signed torsion angles are changed by 2.5°, as shown in the last column of Table 1. We view this small alteration in the torsion angles as acceptable—especially in view of the fact that previous work has used RIS models based on C−C bonds with values of ϕ that differ by as much as 10°.[19−24,27,28] The optimized four-state virtual bond model described by eq 12 and Table 1 is an acceptable model for constraining the coarse-grained beads of *s*PS, when each monomer unit is represented by a single bead placed at the center of mass of the side chain.

The validity of the models at higher temperatures can be assessed by analysis of the temperature coefficient, defined here as $\partial \ln \langle r^2\rangle_0/\partial T$, for the syndiotactic chain. The zeroth-approximation model will have a temperature coefficient of exactly zero because all allowed conformations are equally weighted, regardless of temperature. Therefore, a change in temperature does not affect the average conformation in the zeroth-approximation model. The first-approximation model will

Table 1. Conformations for the Virtual Bond Models of *s*PS, Based on the Interior Virtual Bond in *ldld*-TPN[a]

state	statistical weight for $\mathbf{U}_i$[b]	l_i, nm	θ_i, deg	ϕ_i, deg	optimized ϕ_i, deg
a^0	η^2	0.54	55	180	180.0
b^+	η^2	0.54	78	134	136.5
c^+	1	0.73	78	25	22.5
d^+	η^2	0.54	55	134	136.5
e^+	η^2	0.54	78	87	*c*

[a] ϕ_i for b^-, c^-, d^-, and e^- have the same absolute value, but opposite sign, as ϕ_i for b^+, c^+, d^+, e^+. The second-approximation five-state model uses e^+ and e^-, but the first-approximation four-state model does not. [b] The statistical weights listed are those that appear in successive columns of $\mathbf{U}_{dl,\text{syndio}}$ in eq 12. They are distinct from the statistical weights for individual conformations of *ldld*-TPN, which are individual elements in the first row of $\mathbf{U}_{ld,\text{syndio}}\mathbf{U}_{dl,\text{syndio}}\mathbf{U}_{ld,\text{syndio}}$. [c] Not used in the optimized four-state model.

have a temperature coefficient that is negative. The new conformations introduced in the first-approximation model produce disruptions in the regular conformation of the zeroth-approximation model. These disruptions become more likely as the temperature increases. In terms of the statistical weights, η decreases as T increases. The first-approximation model and the full RIS model both provide disruptions of the regular structure. The temperature coefficient should be negative in both cases, as it is for syndiotactic PS. The first-approximation model incorporates only the most likely disruption of the regular structure. The full RIS model incorporates this disruption and also other less likely disruptions. The only statistical weight in the first-approximation model is η, and so only its temperature dependence determines the value of the temperature coefficient. Four statistical weights (η, ω, ω_x, ω_{xx}) appear in the full RIS model. As T increases, η decreases and the other three statistical weights increase. Therefore, the exact values of the temperature coefficients may differ when calculated using the first-approximation and full RIS models. Based on our first-approximation model, the temperature coefficient is -0.0025 K^{-1} at 300 K. Based on the full RIS model, using the same geometry (tetrahedral bond angles, torsions at 180° and ±60°), it is -0.0021 K^{-1} at 300 K. This illustrative calculation suggests that the difference can be expected in the second significant figure for the temperature coefficient. Similar results can be expected for the case of isotactic PS, while for atactic PS the temperature effect may be diminished since the disruptions in conformation that are caused by increased temperature already exist due to the randomness of the stereochemical sequence.

Before proceeding with applications to PS chains of different stereochemical sequences, it is worthwhile to summarize the strategy used in the treatment of *s*PS. First, the conformations of an appropriate oligomer, TPN, are enumerated. Then an initial, zeroth-approximation model is constructed using only the conformation(s) of the oligomer that have the largest statistical weight. If the zeroth-approximation model is inadequate, as will likely be the case, the conformation(s) with the next highest statistical weight are included in a more elaborate first-approximation model. Then final optimization is achieved by minor adjustment of soft degrees of freedom in the first-approximation model.

Isotactic Polystyrene. The isotactic TPN (*i*TPN) has $Z = 19.9$. Individual conformations have statistical weights that vary by a factor of 10^7. The largest statistical weight, η^3, is shared by four conformations. They account for 79.2% of Z. For *i*TPN with the *dddd* stereochemical sequence, these four conformations are $g^+tg^+tg^+t$, $g^+tg^+ttg^-$, $g^+ttg^-tg^-$, and $tg^-tg^-tg^-$. The first and last conformations are the *tg* helices expected for the isotactic chain. The first helix can be converted into the second, via the g^+ttg^- sequence, where the *tt* is interdiad. Local conformations of higher energy are required to convert the second helix into the first one. A zeroth-approximation model based only on the conformations of *i*TPN of the highest statistical weight must yield $\langle r^2\rangle_0 \sim n^2$ as $n \rightarrow \infty$. When the tg^- conformation is achieved in the *dddd* chain, it propagates indefinitely. An acceptable model must incorporate additional conformations that interrupt the propagation of the tg^- helix in the *dddd* chain or, equivalently, the propagation of the tg^+ helix in the *llll* chain.

The next highest statistical weight, $\eta^4\omega_{xx}$, of *i*TPN is shared by 10 conformations. When these 10 conformations are added to the four conformations considered in the previous paragraph, together they account for 93.3% of Z. These conformations provide many more opportunities for transitions between the *tg* helices, as shown in Table 2. Each of the new conformations has an intradiad *tt* sequence, which causes the appearance of ω_{xx} in the statistical weight. The *tt* conformation of a *meso* diad places the two side chains uncomfortably close to one another, causing the statistical weight to be an order of magnitude smaller than the statistical weight of the most probable conformations.

Table 2. Allowed Disruption and Reformation of *tg* Helices in the Virtual Bond Models for *i*PS, Considered as a String of *d* Pseudoasymmetric Centers

exchange	via	in 4-state model, 79.2% of Z?	in 14-state model, 93.3% of Z?
$g^+t \rightarrow tg^-$	interdiad *tt*	yes	yes
$tg^- \rightarrow g^+t$	intradiad *tt*	no	yes
$g^+t \rightarrow g^+t$	ttt	no	yes
$tg^- \rightarrow tg^-$	ttt	no	yes

Table 3. First-Approximation Virtual Bond Models of Isotactic (*d*) PS Using Conformations of *i*TPN That Account for 93.3% of Z[a]

state	statistical weight for $\mathbf{U}_i$	l_i, nm	θ_i, deg	ϕ_i, deg	optimized θ_i, deg
a^-	η	0.64	70	−58	70
b^-	η	0.64	100	−98	100
c^+	η	0.64	70	98	70
d^+	η	0.64	70	58	70
e^+	η	0.64	101	83	84
f^-	$\eta^2\omega_{xx}$	0.25	140	−38	145
g^0	$\eta^2\omega_{xx}$	0.25	101	0	84
h^+	η	0.64	100	123	100
i^-	η	0.64	70	−83	70
j^-	η	0.64	101	−123	84
k^-	η	0.64	140	−98	145
l^0	$\eta^2\omega_{xx}$	0.25	140	0	145
m^+	$\eta^2\omega_{xx}$	0.25	101	38	84

[a] Signs of all torsion angles are exchanged for isotactic (*l*) PS. The statistical weights listed are those that appear in successive columns of $\mathbf{U}_{dd,\mathrm{iso}}$ in eq 14. They are distinct from the statistical weights for individual conformations of *dddd*-TPN.

The first-approximation RIS model based on the virtual bonds defined by these 14 conformations has $\langle r^2\rangle_0 \sim n$ as $n \rightarrow \infty$. At large n, $\langle r^2\rangle_0$ is 40% larger than the $\langle r^2\rangle_0$ specified by the RIS model based on C−C bonds. This result is obtained using the information in Table 3 and the statistical weight matrix in eq 14. The rows and columns are both indexed in the order a^-, b^-, c^+, d^+, e^+, f^-, g^0, h^+, i^-, j^-, k^-, l^0, m^+. The matrix $\mathbf{U}_{ll,\mathrm{iso}}$ is obtained from $\mathbf{U}_{dd,\mathrm{iso}}$ by exchanging the + and − signs of the torsion angles and the indexes for the rows and columns. In eq 14 and Table 3, we have taken advantage of the fact that two of the new conformations of *dddd*-TPN become indistinguishable when expressed using the virtual bond model, which allows writing $\mathbf{U}$ with 13, rather than 14, rows and columns.

$$\mathbf{U}_{dd,\mathrm{iso}} = \begin{bmatrix}
\eta & \eta & 0 & 0 & 0 & 0 & 0 & 0 & 0 & 0 & \eta & 0 & 0 \\
0 & 0 & \eta & 0 & 0 & 0 & 0 & 0 & 0 & \eta & 0 & 0 & 0 \\
0 & 0 & 0 & \eta & \eta & 0 & 0 & 0 & 0 & 0 & 0 & 0 & 0 \\
0 & 0 & 0 & \eta & \eta & 0 & 0 & 0 & 0 & 0 & 0 & 0 & 0 \\
0 & 0 & 0 & 0 & 0 & \eta^2\omega_{xx} & \eta^2\omega_{xx} & 0 & 0 & 0 & 0 & 0 & 0 \\
0 & 0 & \eta & 0 & 0 & 0 & 0 & 0 & 0 & 0 & 0 & 0 & 0 \\
0 & 0 & 0 & 0 & 0 & 0 & 0 & \eta & \eta & 0 & 0 & 0 & 0 \\
0 & 0 & \eta & 0 & 0 & 0 & 0 & 0 & 0 & \eta & 0 & 0 & 0 \\
\eta & \eta & 0 & 0 & 0 & 0 & 0 & 0 & 0 & 0 & \eta & 0 & 0 \\
0 & 0 & 0 & 0 & 0 & \eta^2\omega_{xx} & \eta^2\omega_{xx} & 0 & 0 & 0 & 0 & 0 & 0 \\
0 & 0 & 0 & 0 & 0 & 0 & 0 & 0 & 0 & 0 & 0 & \eta^2\omega_{xx} & \eta^2\omega_{xx} \\
0 & 0 & \eta & 0 & 0 & 0 & 0 & 0 & 0 & 0 & 0 & 0 & 0 \\
0 & 0 & 0 & 0 & 0 & 0 & 0 & \eta & \eta & 0 & 0 & 0 & 0
\end{bmatrix} \quad (14)$$

Quantitative agreement with the C−C bond based RIS model is improved slightly by incorporating the next most probable conformations in a second-approximation model. These four conformations, each with statistical weight $\eta^3\omega$, allow exchanges between the *tg* helices via interdiad g^+g^- conformations. This model, which now accounts for 97.0% of *Z* for *i*TPN, yields $\langle r^2\rangle_0$ that are 33% larger than the ones obtained with the C−C bond based RIS model at larger *n*.

Rather than seek quantitative agreement between the virtual bond based RIS model and the parent C−C bond based RIS model via including additional conformations, it is preferable to seek agreement within the framework of the first approximation model described in Table 3 and eq 13, by minor adjustments in the conformations that interrupt the *tg* helices. Insight into the soft degrees of freedom that are candidates for distortion is provided by the values of l_i in Table 3. Four l_i have a value of 0.25 nm, which is much smaller than the value of σ for toluene, which has been reported as 0.5932 nm.[26] These short l_i appear in *tt* conformations of a *meso* diad, thereby positioning two side chains in close proximity when the C−C−C angle is tetrahedral and the torsion angles at the C−C bonds are 180°. RIS models based on C−C bonds often alleviate this repulsion somewhat by opening up the C−C−C bond angles slightly (2−4°) and by shifting the torsion angle slightly (5−10°).[23,24] Nevertheless, a repulsive second-order interaction of these side chains cannot be avoided in the *tt* state. This repulsion is responsible for the appearance of ω_{xx} in the statistical weight of these conformations, as in seen the 1,1 element in the statistical weight matrix in eq 7 and in columns 6, 7, 12, and 13 of $\mathbf{U}_{dd,\mathrm{iso}}$ in eq 14. None of the other elements in $\mathbf{U}_{dd,\mathrm{iso}}$ contain any of the ω's in their statistical weight. We postulate that the chain geometry associated with the conformations of virtual bonds that have ω_{xx} in their statistical weights are a reasonable place to make the changes required for optimization of the values of $\langle r^2\rangle_0$ obtained with the first-approximation virtual bond model. We adjust the angles between successive virtual bonds for isotactic triads in the $(tt)(tg^-)$, $(tt)(g^+t)$, $(g^+t)(tt)$, and $(tg^-)(tt)$ conformations. The unadjusted angles were either 101° or 140°. Changing these angles to 84° and 145° produces $\langle r^2\rangle_0$ that are indistinguishable at large *n* for the virtual bond based and parent C−C bond based RIS models. Of course, this particular set of optimized values, which is presented in the last column of Table 3, is not unique. Other bond angles could have been adjusted in the optimization.

Although this procedure leads to a virtual bond RIS model for *i*PS that accurately reproduces the values of $\langle r^2\rangle_0$ from the parent C−C bond based RIS model, it is less satisfying than the equivalent treatment of *s*PS. The *i*PS requires the use of more conformations from TPN and a larger statistical weight matrix. There are two reasons for this difference in the results for *i*PS and *s*PS. First, *s*TPN has a single dominant conformation, with statistical weight η^6, but the largest statistical weight for *i*TPN, η^3, is shared by four conformations. More importantly, the next highest statistical weights (η^4 and $\eta^4\omega_{xx}$, respectively) are found in only three conformations of *s*TPN, but they are found in 10 conformations of *i*TPN. It would be arbitrary to include some of the conformations of *i*TPN with statistical weight $\eta^4\omega_{xx}$ but ignore other conformations with the same statistical weight. Since at least some of these conformations are required for disruption of the dominant *tg* helices, all such conformations are combined with the dominant four conformations, leading to the large (but fortunately sparse) statistical weight matrix in eq 14. This single matrix plays the same role that $\mathbf{U}_d\mathbf{U}_{dd}$ would play in an RIS model based on C−C bonds.

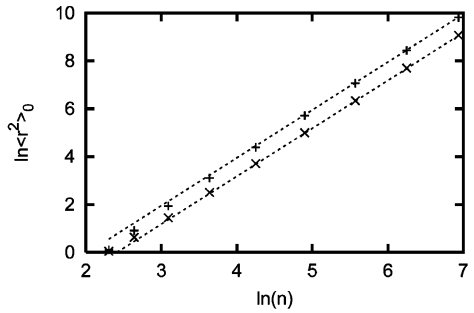

Figure 3. Demonstration that $\langle r^2\rangle_0 \sim n^2$ as $n \rightarrow \infty$ for the zeroth-approximation for PS with $p_m = 0$ (+) and $p_m = 1$ (×). The straight lines have a slope of 2.

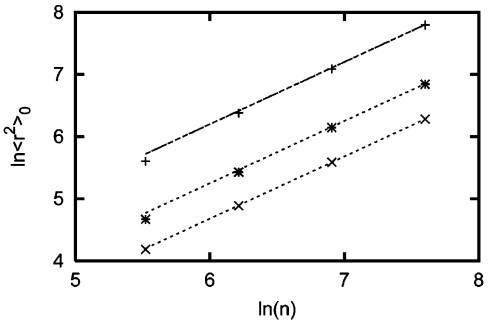

Figure 4. Demonstration that $\langle r^2\rangle_0 \sim n$ as $n \rightarrow \infty$ for the zeroth-approximation for PS with $p_m = 0.1$ (+), $p_m = 0.5$ (×), and $p_m = 0.9$ (*). The straight lines have a slope of 1.

Table 4. Number of Conformations from the Stereoisomers of TPN, and Their Fraction of *Z*, Used in the Construction of the Zeroth- and First-Approximation Virtual Bond RIS Models for *a*PS

stereochemical sequence	no. of conformations		fraction of *Z*	
	zeroth	first	zeroth	first
dddd (mmm)	4	14	0.792	0.933
dddl (mmr)	3	4	0.595	0.725
ddld (mrr)	2	5	0.709	0.922
ddll (mrm)	4	5	0.791	0.870
dlld (rmr)	2	4	0.614	0.856
dldl (rrr)	1	4	0.375	0.826

Atactic Polystyrene. Construction of the virtual bond RIS model for *a*PS begins with the enumeration of all 64 conformations for each of the six unique stereochemical sequences of TPN. As noted above, the highest statistical weight is obtained with only one conformation in *s*TPN, but it is shared by four conformations in *i*TPN. For the remaining stereochemical sequences, this number is 2, 2, 3, and 4 conformations respectively for *dlld*-TPN, *ddld*-TPN, *dddl*-TPN, and *ddll*-TPN. These conformations account for 61.4, 70.9, 59.5, and 79.1% of *Z*, respectively, for these four molecules, as shown in Table 4. The zeroth-approximation virtual bond RIS model combines these conformations with the single conformation that was of highest statistical weight for *s*TPN, and the four conformations that shared the highest statistical weight for *i*TPN.

The zeroth approximation fails badly in the limits where $p_m \rightarrow 0$ or $p_m \rightarrow 1$ because it produces $\langle r^2\rangle_0 \sim n^2$, as shown in Figure 3. Nevertheless, a significant result follows from the examination of how the zeroth approximation behaves at intermediate values of p_m, assuming Bernoullian statistics for the stereochemical sequences. There is a qualitative change in the behavior of $\langle r^2\rangle_0$ when p_m is neither 0 nor 1, but instead has an intermediate value. In the limit as $n \rightarrow \infty$, $\langle r^2\rangle_0 \sim n$ when $0 < p_m < 1$, as shown in Figure 4, whereas $\langle r^2\rangle_0 \sim n^2$ when p_m is 0 or 1, as in Figure 3. The quenched randomness imposed on the stereochemical sequences of the chains when $0 < p_m <$

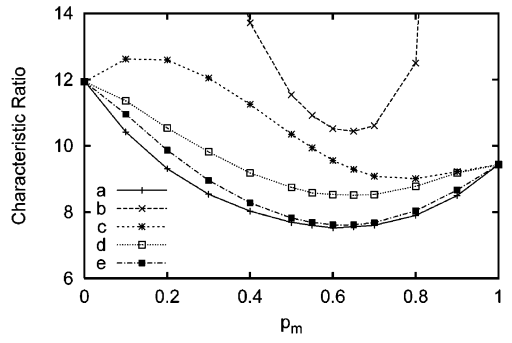

Figure 5. Characteristic ratios for chains of 1000 C−C bonds (500 virtual bonds) and Bernoullian stereochemical sequences. (a) Full RIS model based on C−C bonds. (b) Zeroth-approximation virtual bond model, using only the conformation(s) of highest statistical weight for each stereoisomer of TPN. (c) Improvement of the zeroth-approximation virtual bond model by use of the optimized models for *s*PS and *i*PS. (d) First-approximation model using all conformations with the highest, and second-highest, statistical weights in each stereoisomer of TPN, along with optimization for *s*PS and *i*PS. (e) Optimization, by 2° shifts, for torsion angles unique to *dddl*-, *ddld*-, *ddll*-, and *dlld*-TPN.

1 is sufficient to induce an important qualitative change in the asymptotic behavior of the mean-square dimensions, even though no diad is allowed to occupy any conformation other than those that have the highest statistical weight in the relevant TPN. This restriction on the number of conformations produces $\langle r^2\rangle_0 \sim n^2$ for the stereochemically pure chains. However, any mixing of stereochemical sequences, which happens when $0 < p_m < 1$, is sufficient to produce a different limiting behavior, $\langle r^2\rangle_0 \sim n$. The quenched randomness of the stereochemical sequences produces this qualitative change in the limiting behavior of the unperturbed dimensions in the zeroth-approximation model.

More detailed information on the influence of the quenched randomness is revealed by examination of the characteristic ratios. At each p_m, the values of $\langle r^2\rangle_0$ were calculated for 200 independently generated stereochemical sequences for chains of 1000 C−C bonds (500 virtual bonds), assuming Bernoullian statistics, and then the simple average was obtained from these 200 values. These averages are converted to dimensionless characteristic ratios, C_n, through division by the number of C−C bonds and the square of the length of one such bond. The C_n are compared with similar calculations performed for the parent RIS model based on C−C bonds in Figure 5. As expected, the comparison between the zeroth-approximation and the parent RIS model is awful at the extremes of stereochemical composition. However, the zeroth approximation works surprisingly well at intermediate values of p_m. It yields C_n that are only about 40% too high at the values of p_m which produce the most compact chains. Furthermore, the zeroth approximation correctly captures the fact that the minimum value of C_n is not obtained at $p_m = {}^1/_2$, but is instead displaced toward larger p_m. The quenched randomness of the stereochemical sequences enables the zeroth-approximation model to work surprisingly well at intermediate p_m, especially when contrasted with the dismal failure of the zeroth-approximation model when p_m is either 0 or 1.

The behavior of C_n at the extremes, where p_m is either 0 or 1, can be fixed by replacement of the zeroth approximation for *s*PS and *i*PS by the optimized first-approximation virtual bond treatments that were developed in the previous two sections. The results are depicted as curve c in Figure 5. This new virtual bond model now produces values of C_n for *s*PS and *i*PS that agree with those deduced from the parent RIS model based on C−C bonds. It also reduces the values of C_n for all of the chains, independent of their values of p_m. The smallest value of C_n is still obtained at p_m larger than ${}^1/_2$, and the smallest value of C_n is now about 20% higher in curve c than in curve a. However, on the negative side, C_n now passes through a maximum near p_m of 0.1−0.2, which is contrary to the behavior of the parent RIS model based on C−C bonds, curve a.

The zeroth-approximation model becomes a first-approximation model when the conformations used from each stereoisomer of TPN are those with the first- and second-highest statistical weights for that molecule. The numbers of conformations, and their fraction of Z, are presented in Table 4. The first-approximation model uses either four or five conformations for each TPN except *dddd*-TPN, where the number of conformations is much larger, for the reasons presented above in the discussion of *i*PS. The fractions of *Z* range from 0.725 to 0.933. This first-approximation virtual bond RIS model produces curve d in Figure 3. When compared with curve c, there has been a decrease in C_n at all intermediate values of p_m. The undesirable local maximum, observed near $p_m = 0.1-0.2$ in curve c, is no longer present. The minimum value of C_n is still obtained when p_m is slightly larger than ${}^1/_2$, and this minimum value of C_n is now only 13% larger than the minimum value obtained using the full RIS model based on C−C bonds, curve a.

Agreement can be improved by minor adjustments in the torsion angles that are unique to the virtual bond models for *dddl*-, *ddld*-, *ddll*-, and *dlld*-TPN. No additional adjustments are made in the geometry for the *dddd*- and *dldl*-TPN because these geometries were already optimized for *s*PS and *i*PS in the previous two sections. If these new adjustments are merely 2°, curve d is converted to curve e in Figure 5. The minimum value of C_n in curve e is only 1% larger than the minimum C_n in curve a.

The calculations for curve e in Figure 5 used 32 statistical weight matrices, $\mathbf{U}_{abcde}$, where each letter of *abcde* may be either *d* or *l*. The rows are indexed by the conformations for *abcd*, and the columns are indexed by the conformations for *bcde*, where only the conformations of highest, and second highest, statistical weight are retained for each stereoisomer of TPN. The matrices have either 4 or 5 rows and columns unless the current or previous conformations are for an isotactic sequence, in which case the statistical weight matrix must be larger, in view of the dimensions of the matrix in eq 14. The statistical weight matrices are sparse, with 76% of the elements being null. A few matrices contain a null row or column. This situation arises when an allowed (first-approximation) conformation of the last four torsion angles in TPN with stereochemical sequence *abcd* is not also an allowed conformation (first-approximation) of the first four torsion angles in TPN with stereochemical sequence *bcde*. This effect has been incorporated in the calculations presented here.

The parameters in the virtual bond model for PS may change slightly if they are derived from another RIS model that uses slightly different geometric parameters for this polymer. The alterations in the lengths of the virtual bonds, angles about virtual bonds, and absolute values of the torsions about the virtual bonds in the unoptimized first-approximation model were determined when the bond angles in the underlying RIS model change from tetrahedral to 112° at $CC^{\alpha}C$ and 114° at the C^{α}-CC^{α}, and also the torsions about the C−C bond are displaced slightly from ±60° and 180°, using $\Delta\phi = 10°$. Table 5 shows that the standard deviation of the changes is much larger than the average, signifying that the changes occur in both directions. The most important average change is the increase in the angle between virtual bonds, which will tend to increase the mean-square unperturbed dimensions. This tendency will be reinforced slightly by the average increase in the length of a virtual bond.

Table 5. Changes in Geometry of the Unoptimized First-Approximation Virtual Bond Model When Backbone Bond Angles Are Reassigned at 112° at CC$^{\alpha}$C and 114° at the C$^{\alpha}$CC$^{\alpha}$ and the Torsions Are Reassigned Using $\Delta\phi = 10°$

	change in l, nm	change in θ, deg	change in $\|\phi\|$, deg
average	0.015	2.0	−1.0
standard deviation	0.034	6.4	15.2

A complete description of all of the statistical weight matrices used in the calculations for curve e in Figure 5, including the values of l_i, θ_i, ϕ_i, and the statistical weight for each state, is presented in the Supporting Information. The values of l_i, θ_i, and ϕ_i in the optimized virtual bond model will change somewhat if the torsion angles in the parent C−C bond based RIS model are adjusted away from ±60° and 180° or if the C−C−C bond angles in the backbone are opened slightly, such as to alternating values of 112° and 114°, as is often done.[23,24]

Conclusions

The importance of the quenched randomness of the stereochemical sequences in *a*PS can be assessed by analysis of ensembles that include those conformations of highest statistical weight for every chain. These ensembles, named the zeroth-approximation above, show behavior that depends qualitatively on the value of p_m: $\langle r^2\rangle_0 \sim n^2$ as $n \rightarrow \infty$ if p_m is either 0 or 1, but $\langle r^2\rangle_0 \sim n$ as $n \rightarrow \infty$ when $0 < p_m < 1$. The quenched randomness at intermediate p_m is sufficient to produce this qualitative change in behavior. It is also sufficient to produce a surprising degree of accuracy in the sizes of $\langle r^2\rangle_0$ for the most compact chains. The unperturbed dimensions pass through a minimum at nearly the correct value of p_m, and the $\langle r^2\rangle_0$ at the minimum is in error by only 40%. It is surprising that such a simple model, which considers only the conformations of highest statistical weight for each stereochemical sequence and completely ignores competing conformations of slightly lower probability, can produce such good agreement with the results from the full RIS model based on the C−C bond. This achievement of the simple model is testimony to the profound influence of the quenched randomness on the mean-square dimensions of atactic chains.

Optimized first-approximation virtual bond RIS models, based on the most dominant and second most dominant conformations of each tetrad, can accurately reproduce the mean-square dimensions obtained by a classic RIS model based on C−C bonds. These virtual bond models can serve as constraints on coarse-grained models of atactic polymers with bulky side chains. The precise details of the models will depend on the C−C based RIS model chosen for their generation, but the method introduced here should be applicable in many cases.

Acknowledgment. This research was supported by National Science Foundation Grant DMR0455117 and by the Collaborative Center in Polymer Photonics, which is funded by the Air Force Office of Scientific Research and Wright Patterson Air Force Base.

Supporting Information Available: The statistical weight matrices and geometry (l_i, θ_i, ϕ_i) for the optimized first-approximation virtual bond RIS model of *a*PS. This material is available free of charge via the Internet at http://pubs.acs.org.

References and Notes

(1) Flory, P. J. *Statistical Mechanics of Chain Molecules*; Wiley: New York, 1969; p 232.
(2) Soteros, C. E.; Whittington, S. G. *J. Phys. A: Math. Gen.* **2004**, *37*, R279.
(3) Edwards, S. F.; Vilgis, T. A. *Rep. Prog. Phys.* **1988**, *51*, 243.
(4) Tanaka, F.; Edwards, S. F. *J. Phys. F: Met. Phys.* **1980**, *10*, 2769.
(5) Baschnagel, J.; Binder, K.; Doruker, P.; Gusev, A. A.; Hahn, O.; Kremer, K.; Mattice, W. L.; Müller-Plathe, F.; Murat, M.; Paul, W.; Santos, S.; Suter, U. W.; Tries, V. *Adv. Polym. Sci.* **2000**, *152*, 41.
(6) Doruker, P.; Mattice, W. L. *Macromolecules* **1997**, *30*, 5520.
(7) Flory, P. J. *Statistical Mechanics of Chain Molecules*; Wiley: New York, 1969.
(8) Mattice, W. L.; Suter, U. W. *Conformational Theory of Large Molecules. The Rotational Isomeric State Model in Macromolecular Systems*; Wiley: New York, 1994.
(9) Rehahn, M.; Mattice, W. L.; Suter, U. W. *Adv. Polym. Sci.* **1997**, *131/132*, 1.
(10) Abe, A.; Jernigan, R. L.; Flory, P. J. *J. Am. Chem. Soc.* **1966**, *88*, 631.
(11) Haliloglu, T.; Mattice, W. L. *J. Chem. Phys.* **1998**, *108*, 6989.
(12) Clancy, T. C.; Pütz, M.; Weinhold, J. D.; Curro, J. G.; Mattice, W. L. *Macromolecules* **2000**, *33*, 9452.
(13) Clancy, T. C.; Jang, J. H.; Dhinojwala, A.; Mattice, W. L. *J. Phys. Chem. B* **2001**, *105*, 11493.
(14) Cho, J.; Mattice, W. L. *Macromolecules* **1997**, *30*, 637.
(15) Percec, V.; Ahn, C.-H. Cho, W.-D.; Jamieson, A. M.; Kim, J.; Leman, T.; Schmidt, M.; Gerle, M.; Möller, M.; Prokhorova, S. A.; Sheiko, S. S.; Cheng, S. Z. D.; Zhang, A.; Ungar, G.; Yeardley, D. J. P. *J. Am. Chem. Soc.* **1998**, *120*, 8619.
(16) Schlüter, A. D.; Rabe, J. P. *Angew. Chem., Int. Ed.* **2000**, *39*, 864.
(17) Grayson, S. M.; Frechet, J. M. J. *Macromolecules* **2001**, *34*, 6542.
(18) Flory, P. J. *Macromolecules* **1974**, *3*, 381.
(19) Flory, P. J.; Mark, J. E.; Abe, A. *J. Am. Chem. Soc.* **1966**, *88*, 689.
(20) Williams, A. D.; Flory, P. J. *J. Am. Chem. Soc.* **1969**, *91*, 3111.
(21) Fujiwara, Y.; Flory, P. J. *Macromolecules* **1970**, *3*, 43.
(22) Biskup, U. Cantow, H.-J. *Makromol. Chem.* **1973**, *168*, 315.
(23) Yoon, D. Y.; Sundararajan, P.; Flory, P. J. *Macromolecules* **1975**, *8*, 776.
(24) Rapold, R. F.; Suter, U. W. *Macromol. Theory Simul.* **1994**, *3*, 1.
(25) Humphrey, W.; Dalke, A.; Schulten, K. *J. Mol. Graphics* **1996**, *14*, 33.
(26) Hirschfelder, J. O.; Curtiss, C. F.; Bird, R. B. *Molecular Theory of Gases and Liquids*; Wiley: New York, 1964; p 1213.
(27) Robyr, P.; Müller, M.; Suter, U. W. *Macromolecules* **1999**, *32*, 8681.
(28) Colhoun, F. L.; Armstrong, R. C.; Rutledge, G. C. *Macromolecules* **2002**, *35*, 6032.

MA052434Q